This is an electronic reprint of the original article.
This reprint *may differ* from the original in pagination and typographic detail.

Author(s): Parvez Rana, Benoit St-Onge, Jean-François Prieur, Brindusa Cristina Budei, Anne Tolvanen and Timo Tokola

Title: Effect of feature standardization on reducing the requirements of field samples for individual tree species classification using ALS data

Year: 2022

Version: Published version
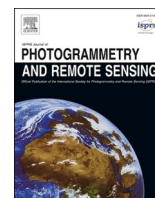
Please cite the original version:

Rana P., St-Onge B., Prieur J.-F., Budei B.C., Tolvanen A., Tokola T. (2022). Effect of feature standardization on reducing the requirements of field samples for individual tree species classification using ALS data. ISPRS Journal of Photogrammetry and Remote Sensing 184: 189-202. https://doi.org/10.1016/j.isprsjprs.2022.01.003.

Effect of feature standardization on reducing the requirements of field samples for individual tree species classification using ALS data

Parvez Rana [a,b,*], Benoit St-Onge [c], Jean-François Prieur [d], Brindusa Cristina Budei [e], Anne Tolvanen [a], Timo Tokola [f]

[a] Natural Resources Institute Finland (Luke), Paavo Havaksen tie 3, 90570 Oulu, Finland
[b] Geography Department, University of Quebec at Montreal, Montreal H3C 3P8, Quebec, Canada
[c] Remote Sensing Consultant, Montreal, Québec, Canada
[d] Département de géomatique appliquée, Centre d'Applications et de Recherches en Télédétection (CARTEL), Université de Sherbrooke, Sherbrooke (QC), Canada
[e] Department of Environmental Sciences, University of Quebec at Montreal, Montreal H3C 3P8, Quebec, Canada
[f] School of Forest Sciences, University of Eastern Finland, P.O. Box 111, FI – 80101 Joensuu, Finland

ARTICLE INFO

ABSTRACT

The objective of this study was to evaluate the effectiveness of three standardization approaches for airborne laser scanning (ALS) feature values used for individual tree species classification. This study is the first effort to assess the transferability of forest tree species classification models derived using monospectral and multispectral ALS data. Three research questions were asked; (1) How do the ALS features differ for the same species in different though comparable ecological regions? (2) How to train a model with one sub-population and apply it in another sub-population? (3) How to fuse models for two areas into a global model? To answer these questions, both 3D and intensity features were extracted from the ALS data from Canadian boreal forests. The ALS feature values were standardized in two different scenarios, disjoint areas, and partially overlapping areas, across three study areas. Feature standardization approaches were used: histogram matching, median-based standardization, and linear regression-based standardization. A linear discriminant analysis (LDA) and random forest (RF) algorithms were employed to classify the study area's major tree species. The Bhattacharyya distance and overall accuracy (OA) were used to assess the classification model performance before and after the feature standardization. Three major conclusions were drawn. First, the Bhattacharyya distance confirmed that intensity features varied across study areas and among tree species, while 3D features were relatively less variable. Second, for the disjoint areas (York Regional Forest (YRF)) and Petawawa Research Forest (PRF)), the feature standardization procedure consistently improved the OA classification for both local model and global model approaches. The feature standardization improved the OA from 16% to 54% using LDA, and from 20% to 55% using RF in the local model. The improvement was from 58% to 66% using LDA, and from 63% to 70% using RF in the global model. It can be concluded that intensity features (at YRF and PRF) were most prone to differ between areas because of scanners and acquisition settings. If ALS data were available from both areas, intensity features need to be normalized so that the local model can be transferred. Finally, for the partially overlapping areas (the northern and southern parts of Black Brook Forest), this study suggests that normalization of ALS data is not needed because they were captured using quite similar ALS settings.

1. Introduction

Tree species information is one of the most requested pieces of information for decision-making in the forest-based industry and ecosystem sciences and management. Currently, species classification relies on traditional manual interpretation of multispectral imagery (visible and infrared bands), which is expensive, time-consuming, and highly uncertain (Budei et al., 2018). The use of airborne laser scanning (ALS) data in recent years has helped the evolution of forest inventory and management techniques. Numerous studies have been published ascertaining the benefits of monospectral ALS features (usually near-infrared: 1064 nm) in the characterization of forest inventory

variables (e.g. height, volume, species composition). Recently, a multi-spectral ALS system (i.e. Titan from Teledyne Optech) has been developed to collect data at different wavelengths (e.g. 532–1550 nm) to enhance the retrieval of forest vegetation dynamics. Few studies have been performed on the use of multispectral ALS data for tree species classification (e.g. Axelsson et al., 2018; Budei et al., 2018; Rana et al., 2018; Yu et al., 2017). These studies all concluded that there were additional gains in tree species classification than monospectral ALS data. Multispectral ALS provides a diversity of spectral information that offers higher reliability and accuracy for individual tree species classification than the single wavelength ALS sensors. Budei et al. (2018) reported an overall accuracy of 76% for ten tree species classification using multispectral ALS data, compared to 65% overall accuracy with monospectral ALS data. Yu et al. (2017) reported 86% overall accuracy for three tree species using multispectral ALS data, compared to 82% overall accuracy with monospectral ALS data.

ALS features are typically categorized into two broad classes, geometric (based on the 3D distribution of returns in the point cloud characterizing a tree) and radiometric (based on return intensity distribution). The addition of different wavelengths in the multispectral ALS system offers more radiometric features than standard ALS. This addition can provide crucial information on tree foliage structure, branching pattern, leaf size, leaf clumping, and foliage density (Korpela et al., 2010b; Shi et al., 2018b). The radiometric features can help to differentiate between tree species because ALS echo properties like echo width are influenced by tree species characteristics.

Tree species classification is challenging in diverse ecosystems due to the presence of a large number of tree species and diverse tree structures. Classification accuracy decreases with the increasing number of tree species (Feret and Asner, 2013), and it is also strongly affected by training sample size (Baldeck and Asner, 2014). Comprehensive training data collection plays a crucial role in tree species classification. For example, Graves et al. (2016) and Freeman et al. (2012) mention the negative impact of small and unbalanced training data on tree species identification. Intra and interspecies feature variation also heighten the challenge for accurate tree species classification. For example, the crown architecture of needleleaf trees (e.g. spruce, balsam fir) is typically vertically extended and spiky compared to the roundish shape of broadleaf trees (e.g. maple, birch, aspen) (Budei et al., 2018). Tree branch orientations also differ between needleleaf and broadleaved trees, causing challenges to the classification accuracy. For example, the orthotropic branch pattern can be seen in Norway spruce and the plagiotropic branch pattern in beech (Millet et al., 1999). Each tree species also differs in its foliage distribution, resulting in diverse architectures. For example, the laser scanning of Norway spruce foliage generates conical crown shapes with clustered ALS points near the stem, while beech generates an ellipsoidal crown shape with an even distribution of ALS points along the stem (Shi et al., 2018b).

Tree species classification has been employed at pixel level (Dalponte et al., 2012), plot level (Sasaki et al., 2012; Van Ewijk et al., 2014), or stand level (Gjertsen, 2007) using various automated or semi-automated methods. However, species are unequivocal only at the single tree level, which makes the approach of individual tree classification more rational and practical. Fassnacht et al. (2016) review found that 56 out of 129 papers (43%) employed an individual tree classification using remote sensing data. However, individual tree level classification could be aggregated at plot-level or stand level when needed. The recent review of Michalowska and Rapinski (2021) mentioned that 80% (out of 97) of studies had four or fewer tree species classified from a single study area. While the first study of individual tree classification based on ALS data was published at the beginning of this century (Holmgren and Persson, 2004), various methodological improvements have been suggested in the last decade. The use of multispectral ALS data for individual tree classification was employed (Budei et al., 2018; Yu et al., 2017), full-waveform ALS data was considered (Blomley et al., 2017; Heinzel and Koch, 2011), and the fusion of ALS with either multispectral (Deng et al.,

2016; Puttonen et al., 2010) or hyperspectral image data (Liu et al., 2017; Shi et al., 2018b) was tested. Alongside the isolation and combination of various classification algorithms such as random forest, neural network, and genetic algorithm were employed and compared (Ko et al., 2014).

Remote sensing-based individual tree classification is an extensively studied subject in the literature. However, most attention has been focused on a single study area at a time. Generalization over multiple areas is particularly difficult due to e.g. need for radiometric correction, differences in the laser's wavelength, system sensitivity and other system properties, and flight parameters (Rana et al., 2018). Theoretically, absolute radiometric calibration concepts are used to produce intensity values which are fully depend only on the target scattering properties. This is necessary for combining large areas covering datasets or multitemporal data from different data acquisition conditions (e.g. Gatziolis, 2011; Hopkinson, 2007; Kaasalainen et al., 2011; Vain et al., 2010; Wagner, 2010). Still, there are many uncertainties in this calibration approach and 3D canopy structure makes the task very complex. Standardization procedures (or relative calibration) are often used to compensate for these difficulties (e.g. Tuomainen and Pekkarinen, 2004), because varying imaging conditions can not be fully modeled using absolute radiometric calibration procedures.

To develop a generalized tree species classification model or to transfer a classifier from one area to another, feature standardization is critical. Feature standardization is a technique to normalize the feature values across multiple areas for developing a generalized tree classifier. The goal of feature standardization is to change the distribution of each feature value to a common scale without distorting differences in the range of feature values. Feature standardization can help to proceed with a generalized model that can be applied to extensive areas with minimal reference data. Feature standardization is also needed to improve model transferability. This study hypothesized that feature standardization allows us to apply a generalized model over different areas if the sampled tree crowns ensure ample coverage of the inter-species variability of the tree crown characteristics across areas. A machine learning classifier trained with the ALS 3D features (also known as geometric features) and intensity features derived from these training crowns should then be able to generate classifications over multiple areas with minimal reference data.

From the modeling perspective, the inventory of an area can be classified using two approaches: (1) a local model: to build a classification model using training crowns of a given area and apply it to another area; the training area must include all possible classes of trees to be classified or (2) a global model: to build a classification model from a training sample pooled from different areas. This study hypothesized that both models could capture the inter-species variability of tree architecture. The practical goal of the models is to minimize field sampling by building a "species multi-area catalog" for training a classifier. These could reduce the necessity of intensive field sampling in each area, and reduce inventory cost and time.

Histogram matching (HM) is a widely used technique in the literature e.g. standardizing ALS intensity values (Ørka et al., 2012), matching multi-temporal ALS points (Nyström et al., 2013), stem volume matching (Baffetta et al., 2012; Gilichinsky et al., 2012), diameter distribution matching (Maltamo et al., 2018; Vauhkonen and Mehtätalo, 2015; Xu et al., 2014) and forest biomass matching (Kauranne et al., 2017)). The above studies concluded that HM assisted in improving the estimation accuracy.

Calibrating a model with a large training sample in each new study area is expected to be more accurate than transferring a model. But recalibration at each location is cost-intensive, a problem which this paper tried to bring a solution by studying how to recalibrate with minimal new training data. The objective of this study was to evaluate standardization approaches for ALS feature values used for individual tree species classification. Our practical goal was to reduce the number of field sample data required for tree species classification. Linear

discriminant analysis and random forest classifier were employed to classify the major tree species in the study area. The different feature categories, 3D or intensity, were tested in the classification, as well as separately or combined to highlight their different response to standardization. The research questions underlying this study are threefold: (1) How do the ALS features differ for the same species in different though comparable ecological regions? (2) How to train a model with one sub-population and apply it to another sub-population (labeled as a local model)? (3) How to fuse two areas into one (labeled as a global model)?

The paper is organized as follows: Section 2 describes the experimental areas and associated ALS data, Section 3 presents the proposed feature standardization method and candidate classification models. In Section 4 and 5, the results of the experiment are presented and discussed. As a final note, Section 6 provides suggestions for future work.

2. Study regions and data

2.1. Study area

The study was conducted in three case study areas: York Regional Forest (YRF, 44.01°N, 79.20°W), Petawawa Research Forest (PRF, 45.59°N, 77.25°W), and Black Brook Forest (BBF, 47.09°N, 67.55°W). YRF and PRF are in Ontario, Canada, whereas BBF is in New Brunswick,

Canada (Fig. 1). YRF is the first public forest in Canada, with 2300 ha, comprised of natural forest (53%), and plantation forest (47%). YRF is composed mostly of needleleaf trees, and ~ 57% of its trees are in the 41–80-years age class (Regional Municipality of York, 2018). PRF has an area of 10,000 ha, and ~ 86% of its trees are in the > 80-years age class (Canadian Institute of Forestry, 2017). Nine tree species (corresponding to eight genera), for a total of 890 tree crowns were sampled for training and validation purposes from YRF (n = 445) and PRF (n = 445) (Table 1). Individual tree species geolocation and species name were recorded during the field survey in the year 2015 and 2016 for YRF and PRF, respectively. The sample crowns were equally divided into two study areas and equally divided into two height stratified classes: <20 m and >=20 m. The geographical distance between YRF and PRF is 260 km. Table 1 shows the statistics of the sample crowns.

BBF is a 200,000-ha forest, in which 40% of the land is spruce plantations (e.g. white spruce, black spruce, and Norway spruce), and 28% of the land is natural broadleaf trees (e.g. sugar maple and yellow birch). The BBF is divided into northern and southern parts for management purposes. The species composition and forest structure are similar in both parts. Needleleaf stands were managed under the selection and shelterwood silvicultural systems for timber production. The remaining forest area contains natural mixed stands of fir and intolerant broadleaf trees (i.e. trees requiring sunlight to maintain vigorous growth). 13 tree species (nine genera), for a total of 3910 tree crowns
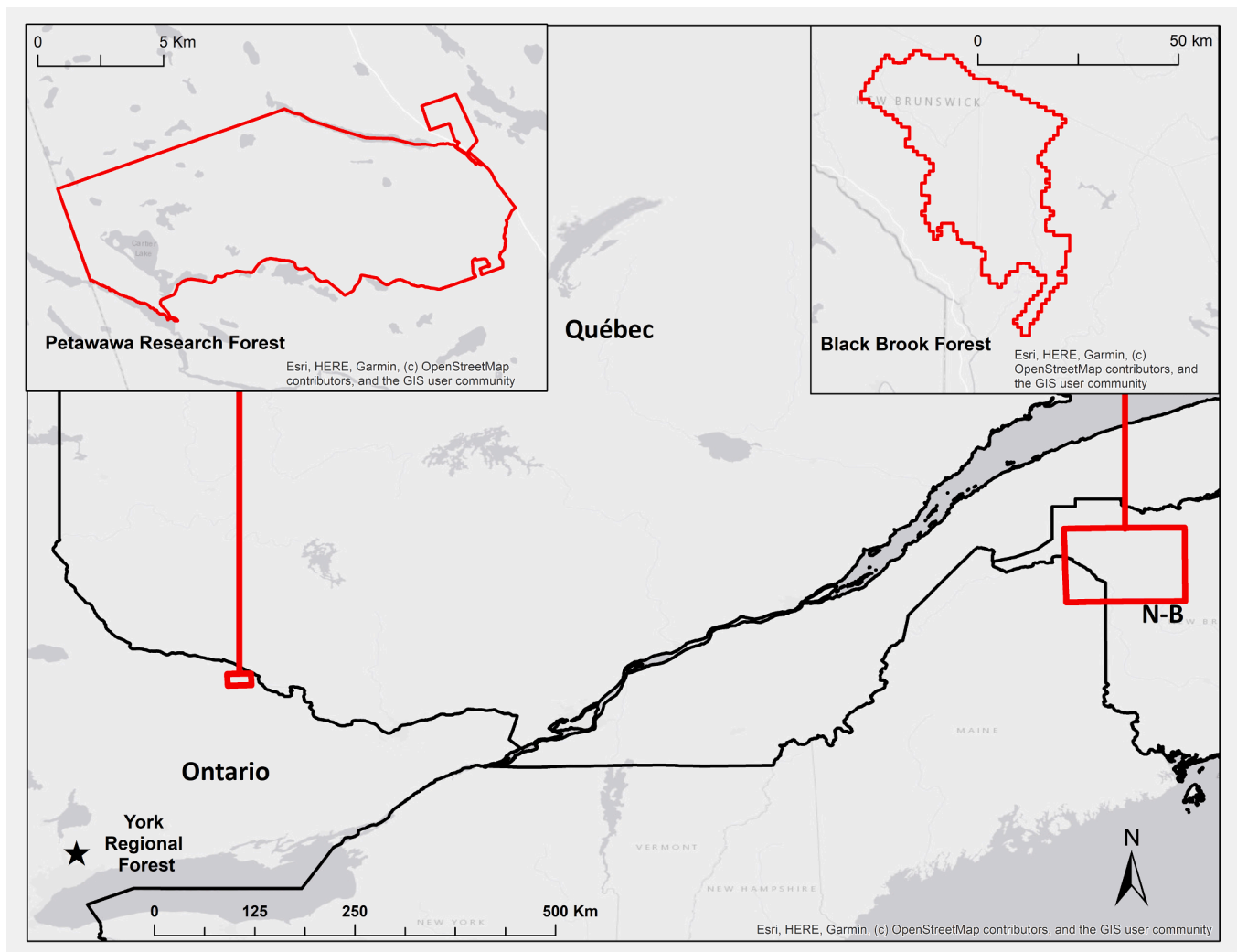

Fig. 1. Location map of the three study areas. The geographical distance between York Regional Forest and Petawawa Research Forest is 260 km. There was no outline polygon for York Regional Forest, because it is composed of several tracts of land that are not altogether.

Table 1

Number and height (m) characteristics of the sample tree crowns (Needleleaf trees = NL, broadleaf trees = BL). / sign was used to separate forest, i.e., YRF/PRF and BBF North/BBF South. N: total number of sample tree crowns.

Forest	BL/NL	Genus	Species	N	Mean	Min	Max
YRF/PRF	NL	*Picea*	*glauca* (white spruce, Sw)	58/58	18.9/20.1	8.3/13.3	28.5/31.4
		Pinus	*strobus* (white pine, Pw)	74/74	22.5/27.6	9.5/9.2	30.8/37.7
			resinosa (red pine, Pr)	86/86	22.5/25.8	4.3/6.6	29.3/35.2
		Larix	*laricina* (american larch, La)	34/34	18.0/17.9	7.7/10.1	28.4/28.6
	BL	*Acer*	*saccharum* (sugar maple, Mh)	70/70	19.9/20.6	10.2/11.5	29.5/28.9
		Betula	*papyrifera* (white birch, Bw)	29/29	17.9/19.7	8.6/15.1	22.3/25.3
		Populus	*tremuloides* (trembling aspen, Pt)	40/40	18.4/21.1	5.2/16.6	27.8/31.2
		Quercus	*rubra* (red oak, Or)	44/44	17.8/19.4	7.9/10.8	26.2/22.7
		Tilia	*americana* (basswood, Bd)	20/20	19.6/21.2	9.6/13.6	28.1/35.0
BBF North /BBF South	NL	*Abies*	*balsamea* (balsam fir, BF)	177/63	12.7/15.5	5.4/5.1	29.8/26.2
		Larix	*laricina* (eastern larch, LA)	100/89	16.6/13.3	5.2/5	25.2/25.4
		Picea	*abies* (Norway spruce, SN)	81/57	14.3/9.8	5.3/5	25.3/15.1
			glauca (white spruce, SW) and *mariana* (black spruce, SB)*	700/49	11.6/19.6	5/5.5	30.2/32.7
		Pinus	*banksiana* (jack pine, PJ)	101/673	15.9/17.6	11.3/13	17.9/20.8
			resinosa (red pine, PR)	136/74	14.1/16.8	11.2/15.4	15.3/18.6
		Thuja	*occidentalis* (eastern white cedar, CW)	51/44	16.1/16.2	9.1/10.8	22.7/27.2
	BL	*Acer*	*rubrum* (red maple, MR)	94/175	18.2/19.5	9.7/5.8	23.3/27.9
			saccharum (sugar maple, MH)	105/190	17.1/18.6	5.1/6.5	26.4/25.7
		Betula	*alleghaniensis* (yellow birch, BY)	120/146	16.3/17.7	8.2/6.3	25.2/26.1
			papyrifera (white birch, BW)	148/116	16.3/15.1	7.2/5.2	24.9/25.1
		Fagus	*grandifolia* (beech, BE)	82/91	15.5/13.9	7.5/5.4	22.6/22.5
		Populus	*tremuloides* (trembling aspen, PT)	112/136	22.1/20.4	8/11	28.4/26.2

* White spruce and black spruce were combined in one group.

were sampled for training and validation purposes from BBF north (n = 2007) and BBF south (n = 1903) (Table 1).

2.2. ALS data

Multispectral ALS data were acquired for YRF and PRF but monospectral ALS data for BBF. In YRF and PRF, the Teledyne Optech Titan system collected data in three different wavelengths: short-wave infrared (SWIR, 1550 nm, Channel(C)1), near-infrared (NIR, 1064 nm, C2) and green (G, 532 nm, C3). The channels have viewing angles of 0° nadir (C2), 3.5° (C1), and 7° (C3) forward-looking. The ALS data acquisition parameters are described in Table 2. For YRF and PRF, the system acquired 3D point clouds (*XYZ*) and intensity (*I*) values in the three wavelengths, i.e. SWIR, NIR, and green. In YRF, aerial photos (10

Table 2

ALS data acquisition parameters.

Characteristics	Petawawa (PRF)	York (YRF)	Black Brook (BBF)	
			North	South
Instrument	Teledyne Optech's Titan	Teledyne Optech's Titan	Riegl LMS-Q680i	Riegl LMS-Q680i
Flight date	July 20, 2016	July 2, 2015	September 8–11, 2011	July 16 – August 1, 2013
Wavelength	532 nm/ 1064 nm/ 1550 nm	532 nm/ 1064 nm/ 1550 nm	1550 nm	1550 nm
Pulse repetition rate (kHz)/channel	300	100	400	400
Scan angle (degree)	30	30	30	30
Flying altitude (above ground, m)	1110	1070	667	600
Average number of first returns m^{-2} of all channels (C1,C2, C3)	13	20.2	5.2	6.5
Average number of first returns m^{-2} by channel (C1, C2, C3) of individual flight lines	4.3, 4.6, 1.6	3.4, 3.4, 3.3	–	–

cm resolution) were also acquired simultaneously with the ALS data. For BBF, Riegl LMS-Q680i ALS data were acquired in two different periods: 2011 for the northern part and 2013 for the southern part. The system acquired 3D point clouds and intensity at near-infrared (NIR: 1550 nm) for BBF.

For YRF and PRF, the vendor provided the range (*RG*) value for each ALS return, which was missing for BBF. The range value for each ALS return of the BBF dataset were calculated using Eq. (1). Then Eq. (2) (Korpela and Rohrbach, 2010) was used for normalizing intensity. Each return intensity value was corrected for YRF, PRF, and BBF.

$$RG = \frac{NFA - Z}{cos\theta} \tag{1}$$

$$I_n = I_{raw} \times \left(\frac{RG}{RG_{ref}}\right)^\alpha \tag{2}$$

where *RG* is the estimated range, *NFA* is the nominal flight altitude above ground, RG_{ref} is the reference range, *Z* is the normalized elevation value of each ALS returns, θ is the angle value for each ALS returns, I_n is range normalized intensity, and I_{raw} is the raw intensity. The α exponent value of 2 was used (Korpela et al., 2010a).

After range normalization, the ALS point clouds were classified into ground returns and vegetation returns (Axelsson, 2000). The ground returns were utilized to produce a raster (0.25-m resolution) digital terrain model (DTM). The *Z* (elevation) values of the ALS returns were normalized by subtracting the elevation of the underlying DTM. A canopy height model (CHM) was generated by assigning the normalized *Z* (elevation) values to each pixel on a raster falling within it. The CHM was utilized for individual tree crown segmentation (see Section 3.1). CHMs created by interpolating the first returns of ALS data typically contain small cavities. The cavities were filled according to the cavity filling algorithm described in St-Onge (2008). This algorithm's fundamental idea was to detect the cavities by a Laplacian filter, fill them using interpolation, and then apply a median filter to the modified pixels to smooth the results. Pixels that are not part of a cavity are left untouched.

3. Methods

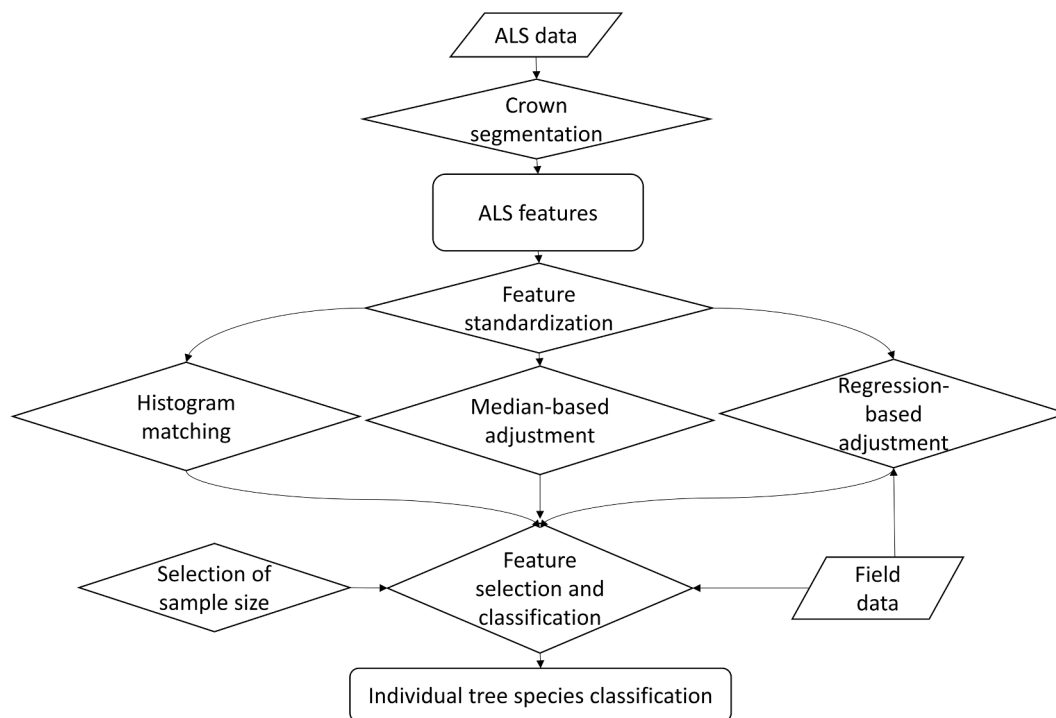The overall workflow, from the initial ALS input data, crown

Fig. 2. Flowchart of the main line of the feature standardization and individual tree classification method.

segmentation and feature standardization to the individual tree species classification, is presented in Fig. 2.

3.1. Crown segmentation

Individual tree crowns for PRF and BBF were delineated using an in-house open-source software, "SEGMA", developed in Python programming language (St-Onge, 2021; St-Onge et al., 2015). The fundamental idea of SEGMA relies on the use of an adaptive Gaussian filter for crown top identification and an auxiliary use of the watershed algorithm for crown boundary delineation. SEGMA calculated a score of between 0 and 100 for each delineated tree crown, indicating the delineation's quality. This score was computed as a weighted mean of centroid distance (i.e. a planimetric distance between XY and the height-weighted centroid) and eccentric, solidity, and coefficient of variation of the CHM height values within the tree crown (St-Onge et al., 2015). The segmented crowns with a delineation score of at least 85 were used for training and validation in PRF and BBF.

Individual tree crowns for YRF were manually segmented using the CHM, intensity images from multispectral ALS, and aerial photos. The manual segmentation was chosen so that species identification accuracy could be assessed without causing significant uncertainty, as with automated segmentation. However, manual segmentation does not guarantee perfect results (Budei et al., 2018). There is a detailed description of YRF crown delineation in Budei et al. (2018). For training and validation purposes at YRF, PRF, and BBF, the sample tree crowns with the following requirements: height ≥ 5 m, area ≥ 1 m^2, and minimum 1 point/channel were used.

3.2. Extraction of ALS features

Feature extraction was categorized into the following two groups, i.e. 3D features and intensity features which were commonly existed in the literature (e.g., Budei et al., 2018; Budei and St-Onge, 2018). The 3D features were calculated from ALS point clouds using the relative XY coordinates for the treetop location and tree height. The 3D features were normalized by the tree height as suggested by Budei et al. (2018,

Holmgren and Persson (2004). The intensity features were calculated from the return intensities in separate channels in the case of multi-spectral ALS.

A total of 136 features was calculated for YRF and PRF, whereas 34 features were calculated for BBF, given the enhanced information produced by multispectral ALS compared to the standard monospectral ALS. A detailed description of each of the features is provided in Appendix A and B (supplementary file). The 3D features included a coefficient of variation of return heights, normalized height percentile (i.e. 25th, 50th, 75th), vegetation points ratio in different height bins, the ratio of the convex hull volume divided by the maximum height cubed, and the slope of the lines linking the apex return to each other return.

Intensity features were comprised of intensity means, the standard deviation, the coefficient of variation, percentiles (5th, 10th, 25th, 50th, 75th, 90th, 95th), the ratio between different features, and the ratio of ALS returns in two channels (e.g. green 532 nm/SWIR 1550 nm) which were calculated for each tree crown. Normalized difference vegetation index (NDVI)-like features were calculated for the multispectral ALS datasets using mean intensity, percentiles at 50th and 75th of green (532 nm), infrared (1064 nm), and SWIR (1550 nm) channels. A detailed description of each of the features is provided in Appendix B.

3.3. Feature standardization

A traditional approach to calibration is to use area-specific models. This approach requires intensive field sample data from each area, which is rigorous, costly, and time consuming. To overcome the above situation, three cross-area standardization approaches were assessed: histogram matching (HM); median-based adjustment (MED); and regression-based adjustment (REG). All the features of the dependent area (PRF and the northern part of BBF) were standardized for the reference area (YRF and the southern part of BBF) using the three approaches mentioned above.

Two different scenarios (disjoint areas: YRF and PRF, partially overlapping areas: BBF north and BBF south) were assessed for feature standardization. In the first scenario, this study postulated that a classifier could be built in one area and then applied to another (i.e.

transferring the model). We assessed the possibility of transferring the model from YRF to PRF. YRF was defined as a reference area, because the crowns were manually delineated using three auxiliary datasets and PRF as a dependent area, which was delineated automatically using watershed segmentation algorithm. In the second scenario, this study postulated that a classifier could be built from training crowns pooled with trees from two areas (i.e. build a global model). A global model was developed using a sample composed of YRF (n = 445) and PRF (n = 445). Similarly, for BBF, a global model was build using a sample composed of the northern (n = 2007) and southern parts (n = 1903) of the study area. The southern part was defined as the reference area and the northern part as the dependent area, because the ALS data of BBF were acquired during the summer of 2013 (trees have leaves during the summer) for the southern part and during the fall of 2011 for the northern part (see Table 2).

HM could be a feasible approach for the standardization of the features (i.e. dependent and reference) when the data were acquired in different illuminations, by different sensors, and in different atmospheric conditions. Gonzalez (2018) describes the procedure of HM in detail. The fundamental of HM is the transformation from dependent distribution to reference distribution. HM equalizes the cumulative histogram of the dependent feature distribution with the reference feature cumulative histogram. Let us consider a cumulative histogram for the dependent distribution, $D(x)$, and the reference distribution, $R(x)$. First, the empirical cumulative distribution of the dependent and reference distribution of features was calculated (CDF_d and CDF_r, respectively). Second, the dependent distribution was modified to fit the reference distribution. The idea was to map each value in the dependent (i) distribution to the value in the reference distribution (j) that had the same probability in the desired probability density function, $R(j) = D(i)$.

For MED, the median value per feature and area was calculated. The residue of the median value of a feature between the two areas was added to the dependent area (i.e. $Residue = R_{median} - D_{median}$, where R was the reference area feature value, and D was the dependent area feature value). The study expected that the residue of the median value between the dependent and reference areas would be an intuitive feature of standardization.

For REG, feature standardization was performed based on linear regression per feature per area. REG method used a minimal sample size (e.g., ten samples per tree species) for median value per tree species which was a limitation of the REG feature standardization method. First, a linear model (i.e. $R \sim D$) was fitted between two areas per feature, where D was the dependent area feature median value, and R was the reference area feature median value. Second, the slope of the line (b) and the intercept (a) were extracted from the above linear model. Finally, the feature value of the dependent area was predicted based on the above model and the fitted equation as follows: $Y = a + bX$, where Y is the estimated dependent area feature (new), and X is the dependent area feature value (old). Fig. 3 shows an example of the scatters plot for REG.

3.4. Feature selection

Additional channels (e.g. 532 nm and 1550 nm wavelengths) available in the multispectral ALS system support the creation of crucial intensity features (e.g., NDVI) which improves the accuracy of individual tree species classification model. From the methodological perspective, the classification of diverse tree species with a large set of auxiliary features is not a trivial task due to several obstacles such as high dimensionality (i.e. large number of features and each feature having a range of possible values) and computational complexity (i.e. time and cost) (Dalponte et al., 2012). Classification accuracy could be increased if only useful features were utilized (Millard and Richardson, 2015). A hybrid approach was employed for composing the final set of features in the classification model. First, a correlation filter was used to refine the list of candidate features that was missing in the VSURF variable selection algorithm (see below). The idea of the correlation filter was to
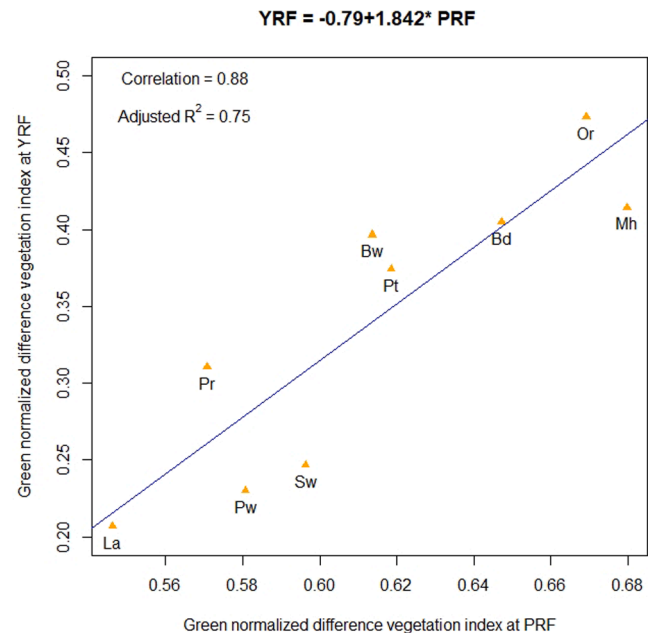

Fig. 3. An example of the scatter plots for regression-based adjustment at Petawawa research forest (PRF) and York regional forest (YRF). Abbreviations of the tree species names are explained in Table 1.

utilize a pair-wise correlation (the cut-off value was 0.9) among the features. *findCorrelation* function (caret package) in R was used for this analysis (R Core Team, 2018). Second, the VSURF (variable selection using random forests package) variable selection algorithm in R (R Core Team, 2018) was employed to select a subset of candidate features. VSURF variable selection was completed in three steps: (1) The mean variable importance (VI) index was used to obtain more stable features from the initial set by removing all the irrelevant features; (2) The less relevant features were further removed based on the mean out-of-bag (OOB) error; (3) This step utilized the mean OOB error, but the features were added to the model stepwise. The main goal in minimizing the number of features was to avoid overfitting and high feature dimensionality. In this study, 8–15 of the most essential features retained in the above steps were forwarded to run in the classification methods.

3.5. Classification methods

Linear discriminant analysis (LDA) and random forest (RF) are well-suited algorithms for individual tree species classification (e.g., Budei and St-Onge, 2018; Budei et al., 2018; Korpela et al., 2010b). This study will not focus on the theoretical background of the above methods. For more detailed information about the above methods, the reader is referred to Breiman (2001) and Fisher (1936). LDA belongs to the parametric family and is a simple algorithm that was used in the classification to highlight the response of tested feature standardization methods. LDA offers class separability by sketching a classification boundary between different classes. RF is a nonparametric algorithm that utilizes the power of ensemble decision trees based on a majority vote for its final classification. RF can also handle the overfitting problem. It is crucial to assess how the feature standardization performance varies in linear LDA and non-linear RF individual tree classification models. The LDA and RF models were developed using the "MASS" and "randomForest" packages in R (R Core Team, 2018). The parameter associated with LDA for each classification model was the equal probabilities across each tree species. The parameters used in the RF classifier for each classification model were 501 decision trees (*ntree*), three predictors at each split (*mtry*), balanced sample (*sampsize*, this
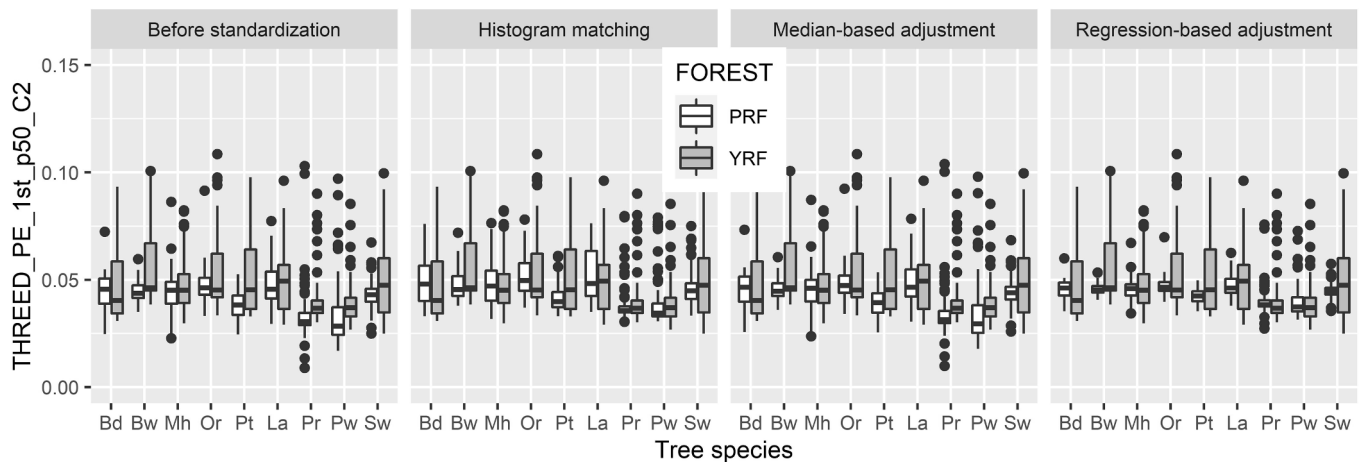
Fig. 4. 3D feature (I) standardization at York Regional Forest and Petawawa Research Forest. THREED_PE_1st_p50_C2 represents the normalized 50th percentile of the first returns in the second Titan channel. Abbreviations of the tree species names are explained in Table 1.

parameter ensured that the numbers to be drawn from the strata at each iteration was the same in each class), and 100 times iterations. LDA and RF classifiers separated the individual tree species using a range of 3D and intensity features, considered separately or together. This grouping was intended to validate the potential of ALS 3D and intensity features for tree species classification.

3.6. Selection of sample size

Each classification model was tested with different sample sizes to assess how feature standardization would affect with different sample sizes, subsequently affecting classification accuracy. The size of the sampled training of 10, 20 (per tree species), and "all" (i.e. all the available sample crowns per tree species) was used. A stratified random sampling procedure was used by utilizing tree species and height as strata criteria to select a subset of the sample (i.e., 10 or 20 per tree species) from all training data. This was implemented using the *strata* function of the *sampling* package (R Core Team, 2018). The same standardized routine was maintained for all areas (i.e. YRF, PRF, BBF). For

YRF and PRF, two height stratified classes, <20 m and ≥20 m, were utilized which helped to sample the trees given the wide range of tree height (from 4.3 m to 38 m) in YRF and PRF. This stratification was proposed because previous studies showed that feature values and classification results might be influenced by tree height (Budei et al., 2018; Budei and St-Onge, 2018). Based on Budei and St-Onge's (2018) suggestion, young and short trees in this study datasets were separated from mature and tall trees using 20 m as an arbitrary tree height threshold. Young and short trees received few ALS points per crown, which creates uncertainty to a feature value within a tree species. On the other hand, mature and tall trees received a high number of ALS points per crown, which stabilizes the ALS feature values within a tree species (Budei and St-Onge, 2018). However, there were not enough samples to consider two height stratified classes, <20 m and ≥20 m, for the northern (2011) and southern (2013) parts of the BBF study area. The process was iterated 30 times with simple random sampling without replacement (*srswor* function of *sampling* package in R statistical programming, R Core Team 2018), and reported the mean and standard deviation of the results.
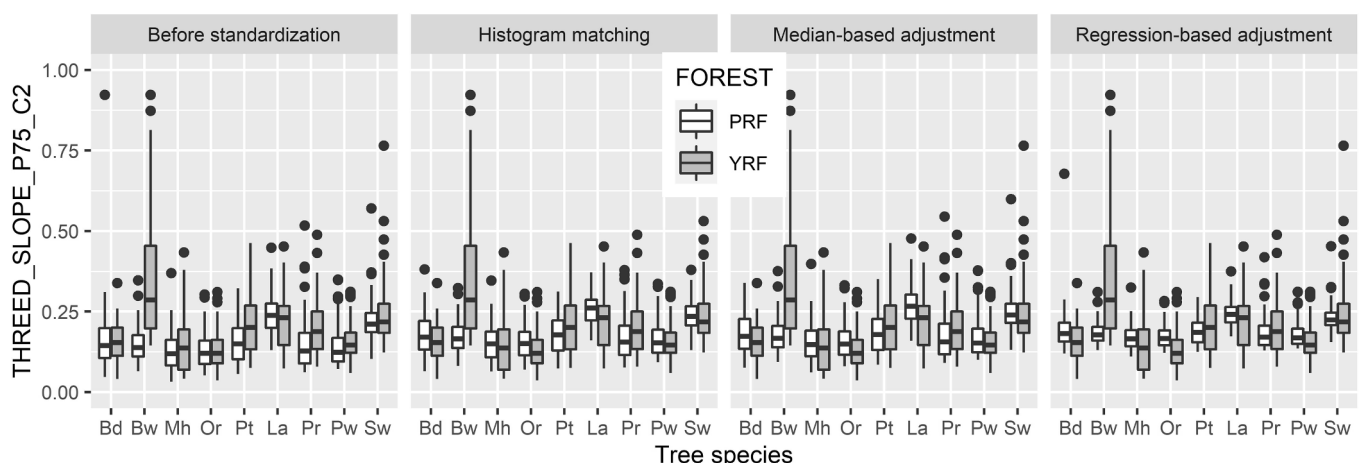

Fig. 5. 3D feature (II) standardization at York Regional Forest and Petawawa Research Forest. THREED_SLOPE_P75_C2 represents the 75th percentile of the slope's values between the highest return in the point cloud and each other return in the second Titan channel. Abbreviations of the tree species names are explained in Table 1.
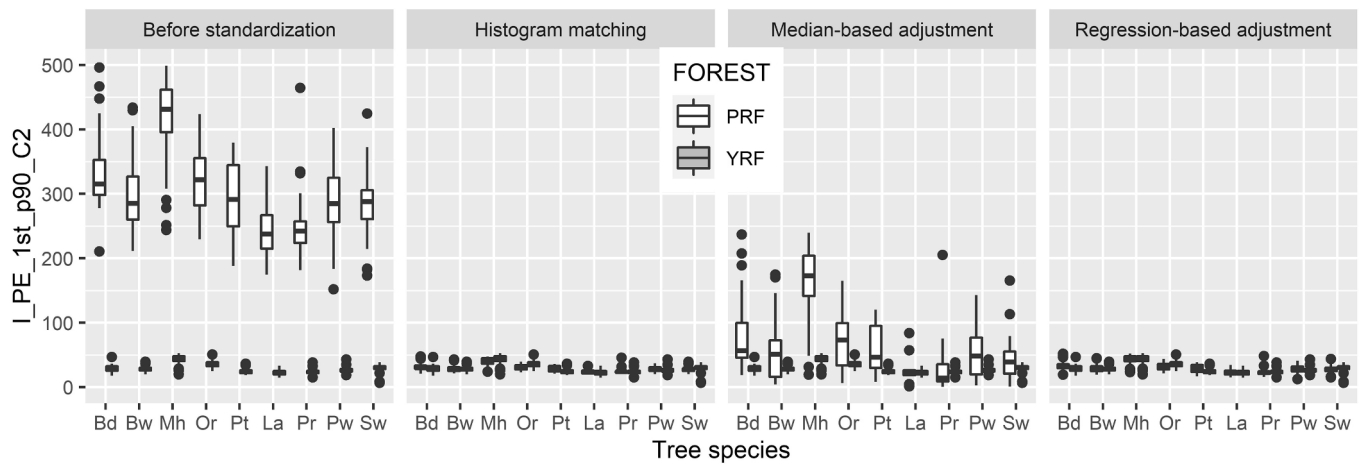
Fig. 6. Intensity feature (I) standardization at York Regional Forest and Petawawa Research Forest. I_PE_1st_p90_C2 represents the 90th percentile of intensity of the first returns of the second Titan channel. Abbreviations of the tree species names are explained in Table 1.
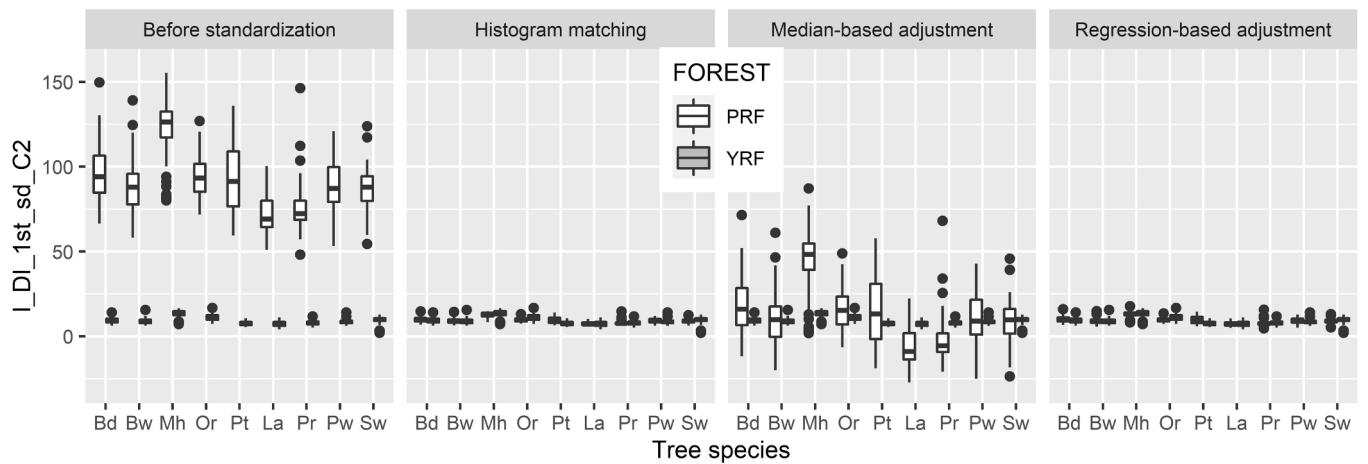
Fig. 7. Intensity feature (II) standardization at York Regional Forest and Petawawa Research Forest. I_DI_1st_sd_C2 represents the standard deviation of the intensity of the first returns of the second Titan channel. Abbreviations of the tree species names are explained in Table 1.
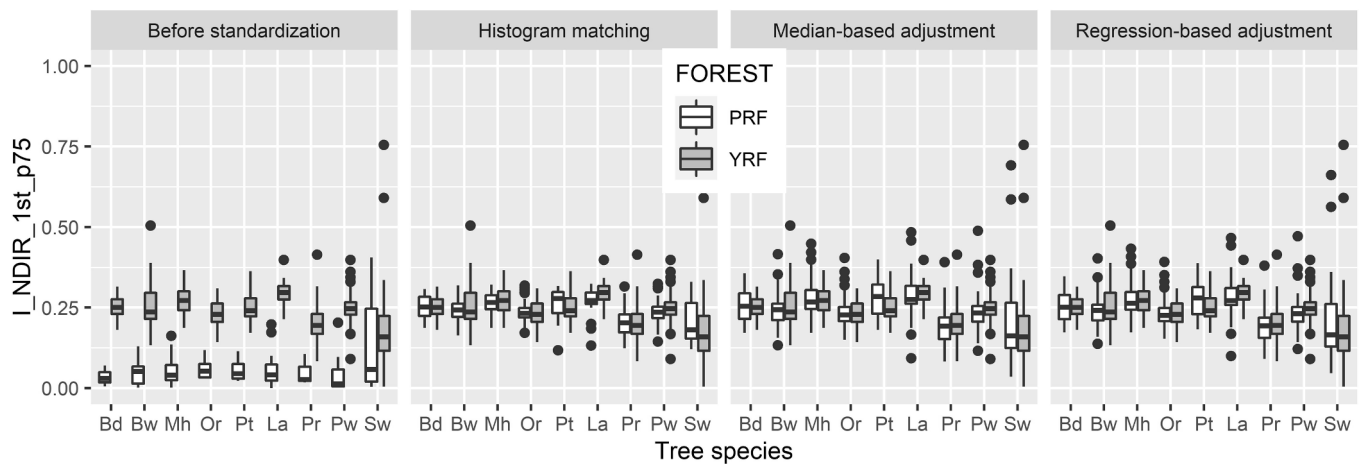
Fig. 8. Intensity feature (III) standardization at York Regional Forest and Petawawa Research Forest. I_NDIR_1st_p75 represents the InfraRed Normalized Difference vegetation index calculated from the 75th percentiles of intensity in the Titan C1:1,550 nm and C3:532 nm. Abbreviations of the tree species names are explained in Table 1.

Table 3
Bhattacharyya distances between feature values at YRF and PRF.

	3D features			Intensity features			All features		
Before standardization	0.130			4.142			1.428		
N/species*	10	20	all	10	20	all	10	20	All
MED	0.215	0.215	0.209	0.394	0.392	0.388	0.130	0.130	0.124
REG	0.595	0.539	0.546	0.130	0.111	0.099	0.445	0.401	0.401
HM	0.114	0.097	0.102	0.097	0.087	**0.065**	0.108	0.094	0.090

* N/species: Number of sample crowns per tree species. The best performing was put in bold.

3.7. Evaluation and performance measures of the standardization

The performance measures of the standardization were evaluated by box plots, scatter plots, Bhattacharyya distance, and overall accuracy. The Bhattacharyya distance is widely used as a measure of divergence between two distributions. The Bhattacharyya distance between two probability distributions P_i and P_j denoted by B_{ij} is defined by

$$B_{ij} = \frac{1}{8}(\mu_i - \mu_j)^T \left(\frac{\sum_i + \sum_j}{2}\right)^{-1}(\mu_i - \mu_j) + \frac{1}{2}\ln\left(\frac{\left|\frac{\sum_i + \sum_j}{2}\right|}{\sqrt{|\sum_i||\sum_j|}}\right) \qquad (3)$$

where μ_i and μ_j refer to the mean of the feature distribution, $\sum_i$, and $\sum_j$ refers to the covariance matrix of the feature distribution. The Bhattacharyya distance will be zero if two feature distributions overlap completely. The Bhattacharyya distance was calculated for (*i*) 3D features, (*ii*) intensity features, and (*iii*) all features. Overall accuracy (OA) was calculated as the total number of the correctly predicted sample divided by the total sample.

4. Results

4.1. Results in disjoint areas, YRF and PRF

Bhattacharyya distances and box plots (Figs. 4–8) confirmed that the intensity features' variability was larger than those of the 3D features before feature standardization (Table 3). The Bhattacharyya distances were reduced after feature standardization between YRF's and PRF's feature values (Table 3).

For the local model (Table 4), both the LDA and RF models had a low OA (16% and 20% respectively) for the classification of nine tree species at PRF before standardization. However, the OA increased using the intensity feature and using all features after feature standardization. For example, the LDA classifier and the RF classifier had an OA of 54% and 55% respectively, using all features and REG feature standardization method, compared to an OA of 20% before standardization (Table 4). However, it is worth noting that 3D features also slightly improved OA after feature standardization. The standardization for the local model needed the smallest number of sample sizes and was also relatively steady with a minimal number of samples (n = 10/species).

Table 4
Overall classification accuracy for the local model at PRF (% average | standard deviation).

		3D features, %			Intensity features, %			All features, %		
LDA	Before standardization	36			16			16		
RF		33			16			20		
N/species*		10	20	all	10	20	all	10	20	All
LDA	MED	45|0.8	45|0.5	44|0	45|0.8	45|0.5	44|0	45|0.8	45|0.5	44|0
	REG	31|5.9	29|6.6	40|0	46|4.8	49|2.4	50|0	52|2.8	54|2.3	54|0
	HM	33|2.1	32|1.5	36|0	37|2.7	36|1.9	50|0	42|1.9	42|1.5	51|0
RF	MED	34|0.7	34.|0.7	34|0	47|0.8	47.|0.4	47|0	49|0.8	50|0.5	48|0
	REG	33|2.9	34|1.2	31|0	50|1.5	51|0.7	52|0	54|1.3	**55|0.8**	**55|0**
	HM	33|1.3	33|0.9	38|0	44|1.5	44|1.1	50|0	44|1.5	44|1.4	53|0

* N/species: Number of sample crowns per tree species. The best performing was put in bold.

Table 5
Overall classification accuracy for the global model at YRF and PRF (% average | standard deviation).

		3D features, %			Intensity features, %			All features, %		
LDA	Before standardization	41			52			58		
RF		50			62			63		
N/species*		10	20	all	10	20	all	10	20	All
LDA	MED	37|0.6	37|0.3	38|0	48|0.6	48|0.4	49|0	61|0.4	61|0.3	62|0
	REG	42|1.0	42|0.9	45|0	59|0.5	59|0.5	60|0	64|0.7	65|0.5	64|0
	HM	42|0.8	42|0.7	42|0	58|0.5	57|0.5	59|0	64|0.6	64|0.6	66|0
RF	MED	47|0.4	46|0.3	48|0	62|0.3	62|0.1	62|0	67|0.3	67|0.1	67|0
	REG	49|0.3	49|0.2	49|0	62|0.3	63|0.1	63|0	69|0.4	69|0.2	69|0
	HM	49|0.5	48|0.5	50|0	64|0.5	63|0.4	64|0	68|0.4	67|0.4	**70|0**

* N/species: Number of sample crowns per tree species. The best performing was put in bold.

Table 6

Bhattacharyya distances between feature values at BBF.

	3D features			Intensity features			All features		
Before standardization	0.078			0.118			0.090		
N/species*	10	20	all	10	20	all	10	20	all
MED	**0.074**	**0.074**	0.084	0.128	0.128	0.111	0.091	0.091	0.093
REG	0.235	0.170	0.094	0.222	0.192	0.150	0.230	0.178	0.113
HM	0.119	0.112	0.116	0.163	0.150	0.115	0.133	0.124	0.116

* N/species: Number of sample crowns per tree species. The best performing was put in bold.

For the global model (Table 5), the OA resulting from the RF classifier increased from 63% before standardization to 66% after feature standardization. A similar improvement of OA resulted from the LDA classifier (Table 5). The improvement of OA was higher using the intensity features than the 3D features. Similar to the local model, the global model was also relatively steady, with a minimal number of samples (n = 10/species) for the feature standardization.

4.2. Results in partially overlapping areas, BBF

The Bhattacharyya distances slightly decreased after feature standardization between feature values at BBF (Table 6) which was also visible in box plots (Figs. 9–12). The OA for the global model at BBF increased but at a minimum level (Table 7). The differences in intensity feature variability between the southern and northern part of BBF and across species were reduced after standardization (Figs. 11–12). The 3D features followed a similar trend (Figs. 9–10). The 3D features were chosen less frequently than the intensity feature by the automatic VSURF algorithm and were used in the classification model. Similar to the disjoint areas, the feature standardization in BBF was also relatively steady, with a minimal number of samples (n = 10/species).
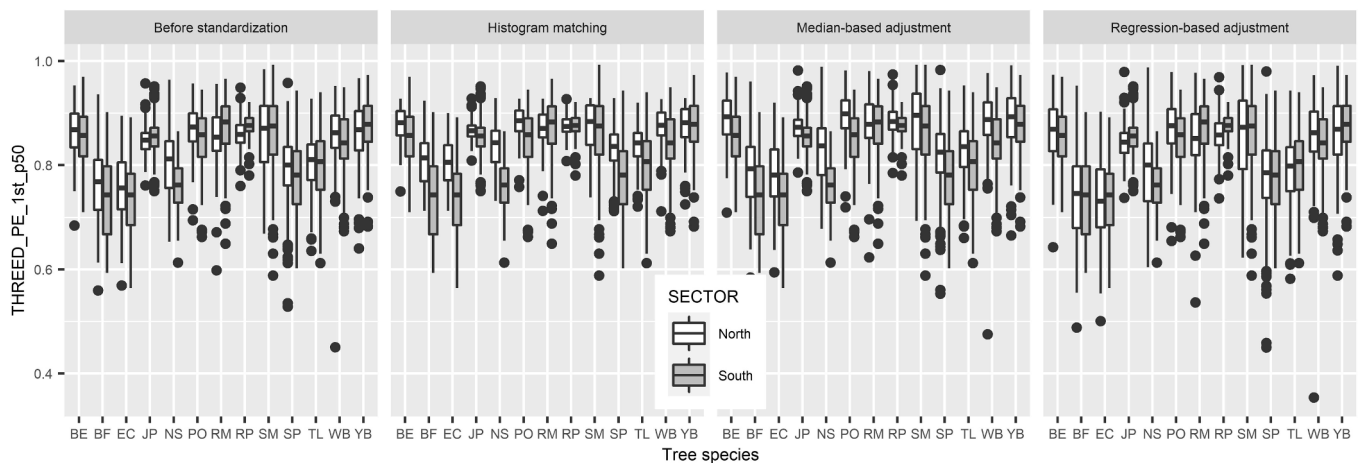

Fig. 9. 3D feature (I) standardization at Black Brook Forest. THREED_PE_1st_p50 represents the normalized 50th percentile of the return height of the first returns. Abbreviations of the tree species names are explained in Table 1.
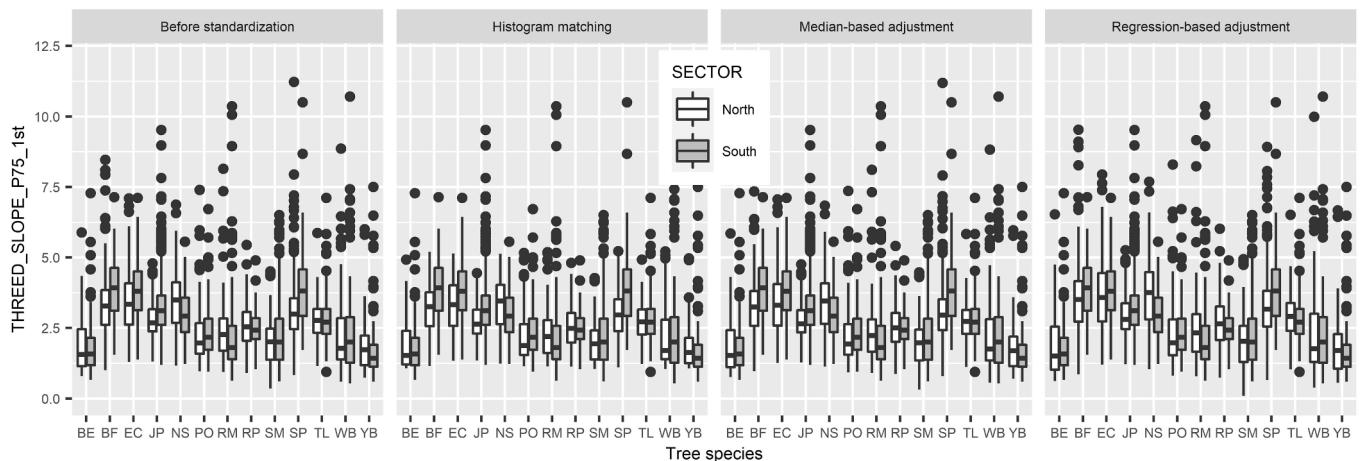

Fig. 10. 3D feature (II) standardization at Black Brook Forest. THREED_SLOPE_P75 represents the 75th percentile of the slope's values between the highest return in the point cloud and each other return. Abbreviations of the tree species names are explained in Table 1.
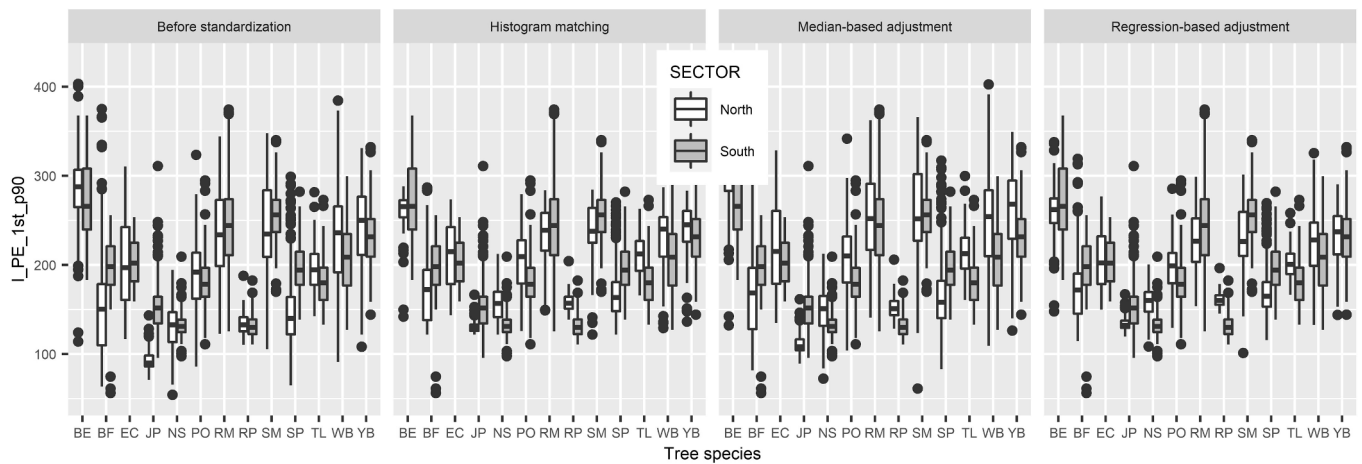
Fig. 11. Intensity feature (I) standardization at Black Brook Forest. I_PE_1st_p90 represents the 90th percentile of the first returns. Abbreviations of the tree species names are explained in Table 1.
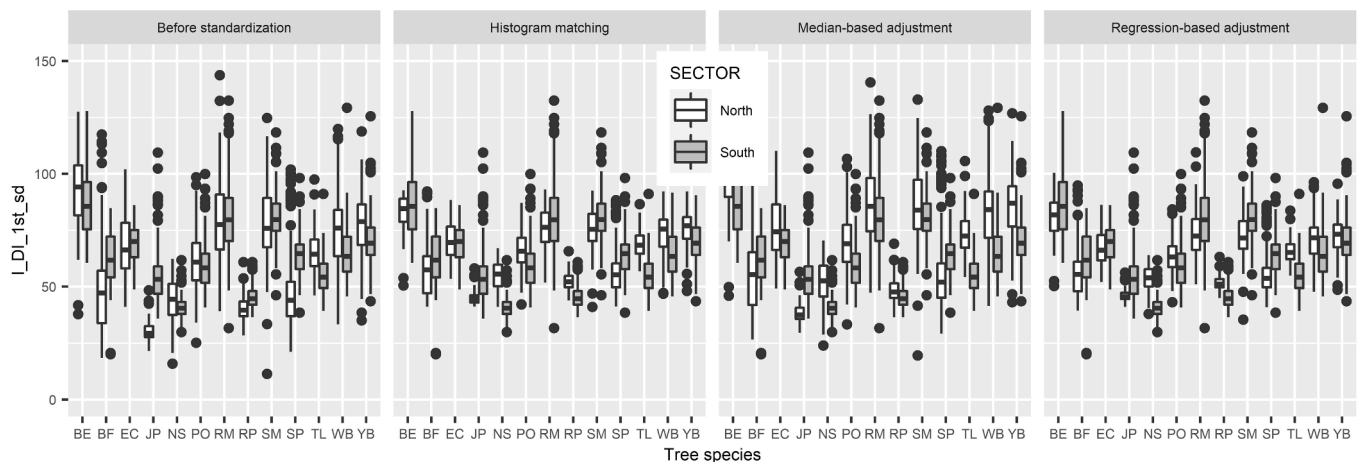

Fig. 12. Intensity feature (II) standardization at Black Brook Forest. I_DI_1st_sd represents the standard deviation of the first returns. Abbreviations of the tree species names are explained in Table 1.

Table 7
Overall classification accuracy for the global model at BBF (% average | standard deviation).

		3D features, %			Intensity features, %			All features, %		
LDA	Before	41			39			47		
RF	standardization	47			45			55		
N/species*		10	20	all	10	20	all	10	20	all
LDA	MED	41|0.6	41|0.4	41|0	36|0.6	36|0.4	37|0	47|0.4	47|0.2	46|0
	REG	42|0.7	42|0.8	42|0	40|0.5	40|0.4	40|0	48|0.5	48|0.5	48|0
	HM	40|1.0	40|0.6	41|0	37|0.5	37|0.4	36|0	46|0.6	46|0.4	47|0
RF	MED	46|0.2	46|0.1	46|0	43|0.4	43|0.3	42|0	54|0.3	54|0.2	54|0
	REG	48|0.6	48|0.5	47|0	49|0.7	49|0.7	49|0	**57**|0.3	56|0.5	56|0
	HM	47|0.3	47|0.2	45|0	46|0.5	46|0.4	42|0	55|0.3	55|0.2	53|0

* N/species: Number of sample crowns per tree species. The best performing was put in bold.

5. Discussion

This study assessed the feature standardization across three study areas to optimize field sampling for species classification at the individual tree level. Two scenarios, i.e. disjoint areas and partially overlapping areas, were assessed that allowed for the scrutiny of the three research questions connected to feature standardization for model transferability. Concerning the *first* research question, the ALS intensity feature varied more compared to those of the 3D features based on the

result from nine individual tree species in YRF and PRF and 13 individual tree species in BBF. Concerning the *second and third* research questions, feature standardization helps to improve the classification accuracy for the local and global models. Results also show that feature standardization can help to minimize the need for extensive sample data collection. This study was the first attempt to demonstrate the transferability of forest tree species classification models derived using monospectral and multispectral ALS data.

This study demonstrates the potential of the transferability of tree

species classification models in both disjoint and partially overlapping areas. Study analysis shows that feature standardization approaches during tree species classification provide several benefits. The first benefit at temporal scale by generating new forest species classification when new ALS data were available. Last benefit at a spatial scale by transferring a local model to another area. The transferability of ALS-based forest tree height and tree volume has been studied by Fekety et al. (2015), Fekety et al. (2018), Karjalainen et al. (2019), Kotivuori et al. (2016), Nilsson et al. (2017), and Tompalski et al. (2019). However, this study's novelty was the use of the feature standardization approach for the tree species transferability model.

The transferability of building a forest tree species classifier was assessed using sample data from one area (YRF) applied to another (PRF) (i.e. a local model). The OA for the local model at PRF increased after feature standardization, indicating that feature standardization played a crucial role. The usability of ALS features for tree species classification was influenced by the ALS acquisition setting. However, tree attributes, e.g. age, site type, and forest management objectives, especially influence tree species classification, while other features may be more invariant (Budei and St-Onge, 2018). On the one hand, factors such as age and site type may have been employed in the tree classification model by providing an extensive training dataset and "black-box classifier" for implicit learning for such dependencies. On the other, the non-standardized ALS feature poses a threat to this implicit learning.

Feature standardization was also assessed in BBF, where ALS data were acquired separately in 2011 for the northern part and in 2013 for the southern part. This study analysis demonstrated that the two different monospectral ALS datasets with a single global modeling approach utilizing feature standardization were capable of classifying 13 tree species in a mixed forest in BBF. The use of local model approach was not attempted, because both areas (northern 2011 and southern 2013) was considered to be a single study area. The Bhattacharyya distance confirmed that both 3D and intensity features varied less at BBF. This was quite expected, as both the northern and southern parts of BBF had similar forest tree composition and structure. This study also found that the feature standardization had contributed to improving the OA for the classification of 13 tree species at BBF, but to a limited extent. The trend was similar for 3D features and intensity features considered separately and together. Both the RF and LDA classifiers showed a similar trend of OA improvement after feature standardization.

Feature standardization increased the OA for the local and global models, although the models were trained with sample tree crowns from two areas (YRF and PRF) 260 km apart. The results showed that intensity features were most prone to change because of scanners and acquisition settings. They needed to be normalized to preserve their capacity to separate species in the local model if we had observations from both areas. In the result from BBF, the intensity features showed a similar response, because the settings in 2011 and 2013 were quite similar, except for the 10% difference in average acquisition height. The BBF results prompted the suggestion that the ALS data did not need feature standardization, because they were captured using a relatively similar setting. Differences in wavelength, system sensitivity, and survey properties may influence the feature values, feature normalization, and models' transferability (Hopkinson, 2007; Hsu et al., 2015; Ussyshkin et al., 2008).

The cost of field sample data collection is of great concern in forest inventory management, because it accounts for most of it (Gobakken and Næsset, 2009; Rana et al., 2016). The variability in forest structure (e.g. height) and composition should be covered in the sample data (Gobakken et al., 2013). The results showed that feature standardization approaches could assist in minimizing the number of samples needed for such a classification across inventory areas. This study found that OA was stable with the small number of samples per tree species (e.g. n = 10) during the feature standardization. For the disjoint areas, the tree height distribution (two classes, i.e. tree height < 20 and > 20) were utilized during the feature standardization. However, for BBF, this study

was unable to utilize the height distribution during the sampling selection of the feature standardization. This study demonstrated the potential of feature standardization, which can help to reduce the major portion of the inventory cost by downsizing the need for field sample data. This study can therefore utilize the findings for future model calibration (including field sample data and ALS data).

Multispectral ALS data have more potential for tree species classification than mono-spectral ALS data. The addition of two wavelength channels to an ALS system offers the possibility of calculating supplementary ALS features, which can then support the calibration of a generalized method of tree species imputation across multiple areas (Rana et al., 2018). Intensity-based features were the most valuable for tree species classification (result not shown), as has previously been observed (Budei et al., 2018; Rana et al., 2018; Shi et al., 2018a; Yu et al., 2017). Among the intensity features, NDVI-like features were the most useful feature in the classification using multispectral ALS data (see also Budei et al., 2018). NDVI features were calculated employing the green channel, which provided chlorophyll content, and the infrared channels provided foliage structure and water content. Among the three channels, the intensity feature of the SWIR channel provided more useful information than the NIR and green channels. Another benefit of SWIR is that it is less prone to noise than other channels (Budei et al., 2018). The laser irradiance at the forest canopy layer in the SWIR channel was higher than the green channel due to the characteristics of SWIR channels (e.g. the lower divergence). The intensity reflectance of the tree foliage at the SWIR channel was also much higher than the green channel (Budei et al., 2018).

6. Conclusion

This study demonstrated a standardization approach for ALS feature values to optimize field sampling for species classification at an individual tree level in three Canadian forests. Three standardization approaches were tested to make feature values of a given species similar between areas. There are three major related conclusions. First, Bhattacharyya distance analysis confirmed that the intensity features (e.g. NDVI vegetation indices) varied to a greater extent than the 3D structural feature before the feature standardization. Second, for the disjoint areas (YRF and PRF), the feature standardization procedure consistently improved classification accuracy for both the local and global models. It could be concluded that intensity features (at YRF and PRF) were most prone to changing (because of scanners and acquisition settings), which need to be normalized so that transferring a local model to another area is possible if observations from both areas were available. Third, for the partially overlapping areas (the northern and southern parts of BBF), this study could suggest that the ALS data did not need to normalize because they were captured using a relatively similar setting. Although the ALS flight parameters were similar, the data were captured in different seasons which probably affects the ALS features. Overall, ALS point cloud characteristics change with changing sensor settings, such as flight height, power, scan angle, and pulse repetition rate. This study, therefore, feels that further studies should be undertaken to confirm this feature standardization approach's validity in other forested landscapes with similar/different ALS sensors and acquisition settings in the large-scale application.

Declaration of Competing Interest

The authors declare that they have no known competing financial interests or personal relationships that could have appeared to influence the work reported in this paper.

Acknowledgements

Appendix A. Supplementary material

Supplementary data to this article can be found online at https://doi.org/10.1016/j.isprsjprs.2022.01.003.

References

Axelsson, A., Lindberg, E., Olsson, H., 2018. Exploring multispectral ALS data for tree species classification. Remote Sens. 10 (2), 183. https://doi.org/10.3390/rs10020183.

Axelsson, P., 2000. DEM generation from laser scanner data using adaptive TIN models. Int. Arch. Photogramm. Remote Sens. 33, 110–117.

Baffetta, F., Corona, P., Fattorini, L., 2012. A matching procedure to improve k-NN estimation of forest attribute maps. For. Ecol. Manage. 272, 35–50. https://doi.org/10.1016/j.foreco.2011.06.037.

Baldeck, C.A., Asner, G.P., 2014. Improving remote species identification through efficient training data collection. Remote Sens. 6, 2682–2698. https://doi.org/10.3390/rs6042682.

Blomley, R., Hovi, A., Weinmann, M., Hinz, S., Korpela, I., Jutzi, B., 2017. Tree species classification using within crown localization of waveform LiDAR attributes. ISPRS J. Photogramm. Remote Sens. 133, 142–156. https://doi.org/10.1016/j.isprsjprs.2017.08.013.

Breiman, L., 2001. Random Forests. Mach. Learn. 45, 5–32. https://doi.org/10.1007/978-3-030-62008-0_35.

Budei, B.C., St-Onge, B., 2018. Variability of Multispectral Lidar 3D and Intensity Features with Individual Tree Height and Its Influence on Needleleaf Tree Species Identification. Can. J. Remote Sens. 44 (4), 263–286. https://doi.org/10.1080/07038992.2018.1478724.

Budei, B.C., St-Onge, B., Hopkinson, C., Audet, F.A., 2018. Identifying the genus or species of individual trees using a three-wavelength airborne lidar system. Remote Sens. Environ. 204, 632–647. https://doi.org/10.1016/j.rse.2017.09.037.

Canadian Institute of Forestry, 2017. Petawawa Research Forest –using 100 years of research to combat climate change. www.cif-ifc.org/. (accessed 25 May, 2020).

Dalponte, M., Bruzzone, L., Gianelle, D., 2012. Tree species classification in the Southern Alps based on the fusion of very high geometrical resolution multispectral/hyperspectral images and LiDAR data. Remote Sens. Environ. 123, 258–270. https://doi.org/10.1016/j.rse.2012.03.013.

Deng, S., Katoh, M., Yu, X., Hyyppä, J., Gao, T., 2016. Comparison of tree species classifications at the individual tree level by combining ALS data and RGB images using different algorithms. Remote Sens. 8 (12), 1034. https://doi.org/10.3390/rs8121034.

Fassnacht, F.E., Latifi, H., Stereńczak, K., Modzelewska, A., Lefsky, M., Waser, L.T., Straub, C., Ghosh, A., 2016. Review of studies on tree species classification from remotely sensed data. Remote Sens. Environ. 186, 64–87. https://doi.org/10.1016/j.rse.2016.08.013.

Fekety, P.A., Falkowski, M.J., Hudak, A.T., 2015. Temporal transferability of LiDAR-based imputation of forest inventory attributes. Can. J. For. Res. 45 (4), 422–435. https://doi.org/10.1139/cjfr-2014-0405.

Fekety, P.A., Falkowski, M.J., Hudak, A.T., Jain, T.B., Evans, J.S., 2018. Transferability of Lidar-derived Basal Area and Stem Density Models within a Northern Idaho Ecoregion. Can. J. Remote Sens. 44 (2), 131–143. https://doi.org/10.1080/07038992.2018.1461557.

Feret, J.-B., Asner, G.P., 2013. Tree species discrimination in tropical forests using airborne imaging spectroscopy. IEEE Trans. Geosci. Remote Sens. 51 (1), 73–84. https://doi.org/10.1109/TGRS.2012.2199323.

Fisher, R., 1936. The use of multiple measures in taxonomic problems. Ann. Eugenics 7, 179–188.

Freeman, E.A., Moisen, G.G., Frescino, T.S., 2012. Evaluating effectiveness of down-sampling for stratified designs and unbalanced prevalence in Random Forest models of tree species distributions in Nevada. Ecol. Modell. 233, 1–10. https://doi.org/10.1016/j.ecolmodel.2012.03.007.

Gatziolis, D., 2011. Dynamic range-based intensity normalization for airborne, discrete return lidar data of forest canopies. Photogramm. Eng. Remote Sensing 77, 251–259. https://doi.org/10.14358/PERS.77.3.251.

Gilichinsky, M., Heiskanen, J., Barth, A., Wallerman, J., Egberth, M., Nilsson, M., 2012. Histogram matching for the calibration of kNN stem volume estimates. Int. J. Remote Sens. 33 (22), 7117–7131. https://doi.org/10.1080/01431161.2012.700134.

Gjertsen, A., 2007. Accuracy of forest mapping based on Landsat TM data and a kNN-based method. Remote Sens. Environ. 110 (4), 420–430. https://doi.org/10.1016/j.rse.2006.08.018.

Gobakken, T., Korhonen, L., Næsset, E., 2013. Laser-assisted selection of field plots for an area-based forest inventory. Silva Fenn. 47, 1–20. https://doi.org/10.14214/sf.943.

Gobakken, T., Næsset, E., 2009. Assessing effects of positioning errors and sample plot size on biophysical stand properties derived from airborne laser scanner data. Can. J. For. Res. 39 (5), 1036–1052. https://doi.org/10.1139/X09-025.

Gonzalez, R., 2018. Digital image processing. Pearson, New York, NY.

Graves, S.J., Asner, G.P., Martin, R.E., Anderson, C.B., Colgan, M.S., Kalantari, L., Bohlman, S.A., 2016. Tree species abundance predictions in a tropical agricultural landscape with a supervised classification model and imbalanced data. Remote Sens. 8, 161. https://doi.org/10.3390/rs8020161.

Heinzel, J., Koch, B., 2011. Exploring full-waveform LiDAR parameters for tree species classification. Int. J. Appl. Earth Obs. Geoinf. 13 (1), 152–160. https://doi.org/10.1016/j.jag.2010.09.010.

Holmgren, J., Persson, Å., 2004. Identifying species of individual trees using airborne laser scanner. Remote Sens. Environ. 90 (4), 415–423. https://doi.org/10.1016/S0034-4257(03)00140-8.

Hopkinson, C., 2007. The influence of flying altitude, beam divergence, and pulse repetition frequency on laser pulse return intensity and canopy frequency distribution. Can. J. Remote Sens. 33 (4), 312–324. https://doi.org/10.5589/m07-029.

Hsu, W.C., Shih, P.T.Y., Chang, H.C., Liu, J.K., 2015. A study on factors affecting airborne LiDAR penetration. Terr. Atmos. Ocean. Sci. 29, 241–251. https://doi.org/10.3319/TAO.2014.12.02.08(EOSI).

Kaasalainen, S., Pyysalo, U., Krooks, A., Vain, A., Kukko, A., Hyyppä, J., Kaasalainen, M., 2011. Absolute radiometric calibration of ALS intensity data: Effects on accuracy and target classification. Sensors 11, 10586–10602. https://doi.org/10.3390/s111110586.

Karjalainen, T., Korhonen, L., Packalen, P., Maltamo, M., 2019. The transferability of airborne laser scanning based tree-level models between different inventory areas. Can. J. For. Res. 49 (3), 228–236. https://doi.org/10.1139/cjfr-2018-0128.

Kauranne, T., Joshi, A., Gautam, B., Manandhar, U., Nepal, S., Peuhkurinen, J., Hämäläinen, J., Junttila, V., Gunia, K., Latva-Käyrä, P., Kolesnikov, A., Tegel, K., Leppänen, V., 2017. LiDAR-Assisted Multi-Source Program (LAMP) for measuring above ground biomass and forest carbon. Remote Sens. 9, 1–36. https://doi.org/10.3390/rs9020154.

Ko, C., Sohn, G., Remmel, T.K., Miller, J., 2014. Hybrid ensemble classification of tree genera using airborne LiDAR data. Remote Sens. 6, 11225–11243. https://doi.org/10.3390/rs61111225.

Korpela, I., Ørka, H., Maltamo, M., Tokola, T., Hyyppä, J., 2010a. Tree Species Classification Using Airborne LiDAR – Effects of Stand and Tree Parameters, Downsizing of Training Set, Intensity Normalization, and Sensor Type. Silva Fenn. 44, 319–339.

Korpela, I., Ørka, H.O., Hyyppä, J., Heikkinen, V., Tokola, T., 2010b. Range and AGC normalization in airborne discrete-return LiDAR intensity data for forest canopies. ISPRS J. Photogramm. Remote Sens. 65 (4), 369–379. https://doi.org/10.1016/j.isprsjprs.2010.04.003.

Korpela, I., Rohrbach, F., 2010. Variation and anisotropy of reflectance of forest trees in radiometrically calibrated airborne line sensor images - Implications to species classification. Int. Arch. Photogramm. Remote Sens. 38, 342–347.

Kotivuori, E., Korhonen, L., Packalen, P., 2016. Nationwide airborne laser scanning based models for volume, biomass and dominant height in Finland. Silva Fenn. 50 (4), 1567. https://doi.org/10.14214/sf.1567.

Liu, L., Coops, N.C., Aven, N.W., Pang, Y., 2017. Mapping urban tree species using integrated airborne hyperspectral and LiDAR remote sensing data. Remote Sens. Environ. 200, 170–182. https://doi.org/10.1016/j.rse.2017.08.010.

Maltamo, M., Mehtätalo, L., Valbuena, R., Vauhkonen, J., Packalen, P., 2018. Airborne laser scanning for tree diameter distribution modelling: A comparison of different modelling alternatives in a tropical single-species plantation. Forestry 91, 121–131. https://doi.org/10.1093/forestry/cpx041.

Michałowska, M., Rapiński, J., 2021. A review of tree species classification based on airborne lidar data and applied classifiers. Remote Sens. 13, 1–27. https://doi.org/10.3390/rs13030353.

Millard, K., Richardson, M., 2015. On the importance of training data sample selection in Random Forest image classification: A case study in peatland ecosystem mapping. Remote Sens. 7, 8489–8515. https://doi.org/10.3390/rs70708489.

Millet, J., Bouchard, A., Édelin, C., 1999. Relationship between architecture and successional status of trees in the temperate deciduous forest. Ecoscience 6 (2), 187–203. https://doi.org/10.1080/11956860.1999.11682520.

Nilsson, M., Nordkvist, K., Jonzén, J., Lindgren, N., Axensten, P., Wallerman, J., Egberth, M., Larsson, S., Nilsson, L., Eriksson, J., Olsson, H., 2017. A nationwide forest attribute map of Sweden predicted using airborne laser scanning data and field data from the National Forest Inventory. Remote Sens. Environ. 194, 447–454. https://doi.org/10.1016/j.rse.2016.10.022.

Nyström, M., Holmgren, J., Olsson, H., 2013. Change detection of mountain birch using multi-temporal ALS point clouds. Remote Sens. Lett. 4 (2), 190–199. https://doi.org/10.1080/2150704X.2012.714087.

Ørka, H.O., Gobakken, T., Næsset, E., Ene, L., Lien, V., 2012. Simultaneously acquired airborne laser scanning and multispectral imagery for individual tree species identification. Can. J. Remote Sens. 38 (2), 125–138. https://doi.org/10.5589/m12-021.

Puttonen, E., Litkey, P., Hyyppä, J., 2010. Individual tree species classification by illuminated-Shaded area separation. Remote Sens. 2, 19–35. https://doi.org/10.3390/rs2010019.

R Core Team, 2018. R: A language and environment for statistical computing. R Foundation for Statistical Computing, Vienna, Austria. URL http://www.R-project.org/.

Rana, M.P., Prieur, J.F., Budei, B.C., St-Onge, B., 2018. Towards a generalized method for tree species classification using multispectral laser scanning in Ontario, Canada. In: IGARSS - 2018 IEEE International Geoscience and Remote Sensing Symposium, pp. 5–8749. https://doi.org/10.1109/IGARSS.2018.8517991.

Rana, P., Gautam, B., Tokola, T., 2016. Optimizing the number of training areas for modeling above-ground biomass with ALS and multispectral remote sensing in subtropical Nepal. Int. J. Appl. Earth Obs. Geoinf. 49, 52–62. https://doi.org/10.1016/j.jag.2016.01.006.

Regional Municipality of York, 2018. York regional forest management plan 2019–2038, Summary May 2018. www.york.ca. (Accessed 25 May 2020).

Sasaki, T., Imanishi, J., Ioki, K., Morimoto, Y., Kitada, K., 2012. Object-based classification of land cover and tree species by integrating airborne LiDAR and high spatial resolution imagery data. Landsc. Ecol. Eng. 8 (2), 157–171. https://doi.org/10.1007/s11355-011-0158-z.

Shi, Y., Skidmore, A.K., Wang, T., Holzwarth, S., Heiden, U., Pinnel, N., Zhu, X., Heurich, M., 2018a. Tree species classification using plant functional traits from LiDAR and hyperspectral data. Int. J. Appl. Earth Obs. Geoinf. 73, 207–219. https://doi.org/10.1016/j.jag.2018.06.018.

Shi, Y., Wang, T., Skidmore, A.K., Heurich, M., 2018b. Important LiDAR metrics for discriminating forest tree species in Central Europe. ISPRS J. Photogramm. Remote Sens. 137, 163–174. https://doi.org/10.1016/j.isprsjprs.2018.02.002.

St-Onge, B., 2008. Methods for improving the quality of a true orthomosaic of Vexcel UltraCam images created using a lidar digital surface model. In Silvilaser 2008, 555–562.

St-Onge, B., 2021. SEGMA: Tree Crown Delineation Software From Lidar Data, https://en.geophoton.ca/téléchargements. (Accessed 30 November, 2021).

St-Onge, B., Audet, F.A., Bégin, J., 2015. Characterizing the height structure and composition of a boreal forest using an individual tree crown approach applied to photogrammetric point clouds. Forests 6, 3899–3922. https://doi.org/10.3390/f6113899.

Tompalski, P., White, J.C., Coops, N.C., Wulder, M.A., 2019. Demonstrating the transferability of forest inventory attribute models derived using airborne laser scanning data. Remote Sens. Environ. 227, 110–124. https://doi.org/10.1016/j.rse.2019.04.006.

Tuominen, S., Pekkarinen, A., 2004. Local radiometric correction of digital aerial photographs for multi source forest inventory. Remote Sens. Environ. 89 (1), 72–82. https://doi.org/10.1016/j.rse.2003.10.005.

Ussyshkin, V., Boba, M., Sitar, M., 2008. Performance characterization of an airborne lidar system: bridging system specifications and expected performance. In: The International Archives of the Photogrammetry, Remote Sensing and Spatial Information Sciences. Vol. XXXVII. Part B1. Beijing 2008.

Vain, A., Yu, X., Kaasalainen, S., Hyyppa, J., 2010. Correcting airborne laser scanning intensity data for automatic gain control effect. IEEE Geosci. Remote Sens. Lett. 7 (3), 511–514. https://doi.org/10.1109/LGRS.2010.2040578.

Van Ewijk, K.Y., Randin, C.F., Treitz, P.M., Scott, N.A., 2014. Predicting fine-scale tree species abundance patterns using biotic variables derived from LiDAR and high spatial resolution imagery. Remote Sens. Environ. 150, 120–131. https://doi.org/10.1016/j.rse.2014.04.026.

Vauhkonen, J., Mehtätalo, L., 2015. Matching remotely sensed and field-measured tree size distributions. Can. J. For. Res. 45 (3), 353–363. https://doi.org/10.1139/cjfr-2014-0285.

Wagner, W., 2010. Radiometric calibration of small-footprint full-waveform airborne laser scanner measurements: Basic physical concepts. ISPRS J. Photogramm. Remote Sens. 65 (6), 505–513. https://doi.org/10.1016/j.isprsjprs.2010.06.007.

Xu, Q., Hou, Z., Maltamo, M., Tokola, T., 2014. Calibration of area based diameter distribution with individual tree based diameter estimates using airborne laser scanning. ISPRS J. Photogramm. Remote Sens. 93, 65–75. https://doi.org/10.1016/j.isprsjprs.2014.03.005.

Yu, X., Hyyppä, J., Litkey, P., Kaartinen, H., Vastaranta, M., Holopainen, M., 2017. Single-sensor solution to tree species classification using multispectral airborne laser scanning. Remote Sens. 9, 1–16. https://doi.org/10.3390/rs9020108.